FOUR- AND FIVE-LAYER SILICON-CLAD DIELECTRIC WAVEGUIDES*

Glen McWright and T. E. Batchman
University of Virginia
Charlottesville, Virginia

ABSTRACT

Computer modeling studies on four-layer silicon-clad planar dielectric waveguides indicate that the attenuation (α) and mode index (β/K) behave as exponentially damped sinusoids as the silicon thickness is increased. The observed effect can be explained as a periodic coupling between the guided modes of the lossless structure and the lossy modes supported by the high-refractive index silicon. Furthermore, the attenuation and mode index are significantly altered by conductivity changes in the silicon. An amplitude modulator and phase modulator have been proposed using these results. Predicted high attenuations in the device may be reduced significantly with a silicon dioxide buffer layer.

INTRODUCTION

A need has arisen for direct optical modulation technology. This need has arisen from the search for faster digital switches, higher capacity data channels, and light, compact data preprocessing equipment for satellites. One promising technology that has been examined is the modulation of a guided light wave via photoconductivity changes in a semiconductor cladding.

Computer modeling studies on four- and five-layer, silicon-clad, planar dielectric waveguides indicate that the propagation characteristics can be altered by changes in the complex permittivity of the silicon and in the thickness of the silicon. Using these predictions, an intensity modulator and a phase modulator based on photon-induced conductivity changes in the semiconductor cladding have been studied.

SEMICONDUCTOR-CLAD WAVEGUIDES

The four-layer planar waveguide structure under consideration is shown in Figure 1, where it is assumed that light is propagating in the dielectric (N_3) and all materials are lossless except for the semiconductor (N_2). We desire to solve for the complex mode propagation constant ($\alpha + j\beta$).

*Research sponsored by NASA-Langley Research Center under Grant NSG-1567.

One technique (1) extends Maxwell's equations and boundary conditions to numerically solve a transcendental equation relating the attenuation constant (α) and phase constant (β) to the material types and thicknesses of the waveguide structure (hereafter refered to as PROGRAM WAVES).

A more efficient method (2) utilizes a matrix representation of Maxwell's equations, field solutions and boundary conditions in each waveguide layer (hereafter refered to as PROGRAM MODEIG). The matrices are multiplied and a characteristic matrix for the entire structure is obtained which yields the attenuation constant and phase constant.

The waveguide consists of a semi-infinite glass substrate, a polystyrene core of thickness 1 micrometer, a silicon cladding of .01 micrometer to 10 micrometers in thickness, and a semi-infinite layer of air. Each material is characterized by a complex relative permittivity, $\hat{\varepsilon}$; a free space wavelength of 632.8 nanometers is assumed and material parameters are shown for this wavelength (Fig. 1) Layers N_1, N_3, and N_4 are lossless dielectrics, so ε_r is real; however, at optical frequencies the permittivity of the silicon (N_2) is complex ($\varepsilon_r = \varepsilon'_r + j\varepsilon''_r$), and the complex part is a linear function of the conductivity ($\varepsilon''_r = \sigma/\omega\varepsilon_o$).

PREDICTED CHARACTERISTICS

The curves presented in Figures 2 and 3 were generated by repeated use of our own PROGRAM WAVES and later confirmed with PROGRAM MODEIG. The silicon cladding was varied from .01 micrometer to 10 micrometers and the complex mode propagation constant was calculated. The expected result was that as the cladding thickness was reduced to zero, the attenuation decreases to zero in a well-behaved manner; however, the results were not well-behaved when the silicon thickness falls below 1 micrometer. The curves are similar to exponentially damped sinusoids. Extreme β/K variations correspond to median values in the α-curve, and extreme α variations correspond to median β/K values. By increasing the conductivity of the silicon cladding, the amplitude of the curve oscillations decreases slightly, and the α-curve shifts vertically to a higher attenuation. The percent change in attenuation compared to dark conditions ($\sigma = \sigma_o$) for different conductivities ($\sigma = 1.1\ \sigma_o$, $\sigma = 1.25\ \sigma_o$, $\sigma = 1.5\ \sigma_o$) is shown in Figure 4. The β/K curves shift for a conductivity change, as well, although not in such a well-defined manner. The percent phase shift compared to dark conditions ($\sigma = \sigma_o$) for different conductivity changes is shown in Figure 5. These effects will be used for intensity and phase modulation in a device where a signal source induces photoconductivity changes in a thin silicon cladding on a waveguide, thus modulating a coherent beam in the guide.

FIELD CALCULATIONS

We now consider the problem of correlating the local maximum/minimum points on the attenuation and mode index curves with the electric and magnetic field distributions in the waveguide layers. Results indicate that the presence of a thin silicon film (<98Å) has little effect on the wave function profiles; the profiles are similar to those of the three-layer lossless structure (air-dielectric-substrate). For the thick silicon film structure, however, the lowest order mode of the lossless three-layer structure couples to the modes associated with the

semiconductor film (the high-refractive index silicon behaves as a waveguide). Furthermore, the coupling between the modes supported by the three-layer lossless structure and the high loss TE' modes* of the silicon waveguide determines the attenuation and phase of the complete four-layer structure.

Our results can be described as periodic coupling between the guided mode and other leaky modes of the same guide. First, we examine the partial structure consisting of a silicon guiding region surrounded by semi-infinite layers of air and polystyrene. The attenuation and mode index are shown in Figures 6 and 7. We note a phase match condition between the modes of the partial structure (air, silicon guide, polystyrene) and the TE_0 mode of the complete waveguide at cutoff thicknesses** for successively higher order modes of the partial structure. The sharp peaks on the attenuation curve, for the four-layer structure, occur whenever the guided wave is strongly coupled into the high-loss modes of the silicon partial structure; conversely, the sharp nulls of apparently zero coupling efficiency occur at thicknesses midway between the values for two adjacent leaky modes of the partial structure. This is similar to the results of power transfer calculations for linearly tapered directional couplers (3, 4). The abrupt transitions on the mode index curve of the complete structure occurs when the phase match condition is satisfied and the guided wave couples into successively higher order modes of the partial structure.

We now consider our results in terms of the electric and magnetic field distributions at the local maximum/minimum points on the attenuation vs. silicon thickness curve. The real part of the TE_0 mode electric field profile in the transverse direction is shown for a cladding thickness, t_2 = .007 micrometers (Figure 8(a)). We recall that this thickness is below the cutoff value for the silicon waveguide structure; note that the wave function profile is not appreciably distorted.

For the first local minimum (t_2 = .05μm), we observe that the field strength at the silicon-dielectric interface approaches zero. We also note the exponentially decaying solutions in the outer, semi-infinite layers as expected. For the first local maximum (t_2 = .09μm), we observe a sharp peak in the wave function profile at the silicon-dielectric interface as coupling to the TE'_1 mode of the silicon guide occurs (Figures 8(b) and 8(c)).

Similar behavior is noted for the next local minimum/maximum pair, Figures 9(a) and 9(b), (t_2 = .13μm and t_2 = .18μm). The field strength is effectively zero at the silicon-dielectric interface for the local minimum, and a sharp peak in the wave function is evident for the local maximum as coupling to the TE'_2 mode of the silicon guide occurs. We also note that the field begins to oscillate in the semiconductor cladding as we couple into the higher order modes of the silicon waveguide structure.

Again, for the next local minimum/maximum pair (t_2 = .22μm and t_2 = .26μm) the number of field oscillations in the silicon increases. (See figures 9(c) and 9(d).) The increase or reduction in field strength at the silicon-dielectric interface is also apparent. At this local maximum (t_2 = .26μm), there is the sharp field peak at the interface, but the field decays rapidly through the dielectric indicating almost complete energy transfer. For the other maxima cases considered, the sharp

---

* TE'_1 denotes guided modes in the semiconductor and TE_i denotes guided modes in the dielectric.

** Cutoff for the silicon guide occurs when $(\beta/K)_{Si} < n_{polystyrene}$.

peak was evident at the interface, however, a sizable field was still present in the polystyrene dielectric. This indicates that the local maximum (and likely, minimum) values used for the calculations are not the precise values as in the former case (Figures 9(a) and 9(b)).

The field plots indicate, then, that the attenuation and mode index of the four-layer structure may be explained quite simply as a coupling between the basic three-layer lossless waveguide (air-dielectric-substrate) modes and the high loss TE' modes of the silicon guide. For a local minimum on the attenuation-thickness curve, the field at the semiconductor interface is zero, and for a local maximum, a sizable field is set up at the interface which decays rapidly through the guide and substrate. Finally, the number of field oscillations in the silicon increases as we couple into the higher order modes of the partial structure.

REDUCTION IN ATTENUATION THROUGH USE OF FIVE-LAYER STRUCTURE

Thin dielectric buffer layers have been used to lower the attenuation losses of metal-clad dielectric waveguides (5). These layers are placed between the dielectric core and the metal, and act as buffers to remove a large portion of the field from the metal claddings. We now consider the effect of an SiO_2 buffer layer on the attenuation vs. silicon thickness characteristics.

The result for an SiO_2 buffer layer ($\varepsilon_r = 2.12$) of several different thicknesses is shown in Figure 10. We note the familiar damped sinusoidal behavior and the corresponding reduction in attenuation.

The result for an SiO_2 buffer layer ($t_{SiO_2} = 2000\text{Å}$) of several different permittivities is shown in Figure 11. Again we note the damped sinusoidal behavior and the corresponding reduction in attenuation.

Our studies indicate, then, that the attenuation may be reduced significantly with an SiO_2 buffer layer while still preserving the oscillatory behavior of the attenuation curve; more effective reduction is accomplished with a lower permittivity buffer layer. Also, a buffer layer increases the β/K values slightly but decreases the amplitude of the oscillations on the β/K-thickness curve.

CONCLUSIONS

Computer modeling studies on four-layer silicon-clad dielectric waveguides indicate that the attenuation (α) and mode index (β/K) behave as exponentially damped sinusoids as the silicon thickness is increased. The observed effect can be explained quite simply as a periodic coupling between the guided modes of the lossless structure and the lossy modes supported by the high-refractive index silicon. Furthermore, the attenuation and mode index are significantly altered by conductivity changes in the silicon; an amplitude modulator and an intensity modulator have been proposed using these results. Predicted high attenuations in the device may be reduced significantly with a silicon dioxide buffer layer between the semiconductor and the polystyrene guide.

Experimental confirmation of the predicted characteristics is still necessary. A number of thin-silicon film waveguides have been RF sputtered but attenuation measurements to verify the damped oscillatory behavior are forthcoming. Conductivity variations of the silicon should demonstrate the modulation capabilities.

REFERENCES

1. Batchman, T.E.: Investigation of Direct Integrated Optics Modulators - Applicable to Data Preprocessors. UVA/528171/EE80/102 (NASA Grant NSG-1567), Univ. of Virginia, Mar. 1980. (Available as NASA CR-162894)

2. Smith, Robert G., and Mitchell, Gordon C., "Calculation of Complex Propagating Modes in Arbitrary, Plane-Layered Complex Dielectric Structures", E.E. Tech. Report No. 206, University of Washington, National Science Foundation Grant; Eng. 76-09937.

3. Jones, Alan L., "Coupling of Optical Fibers and Scattering in Fibers", J. Opt. Soc. Amer., Vol. 55, No. 3, March 1965, pp. 261-71.

4. Smith, Robert B., "Analytic Solutions for Linearly Tapered Directional Couplers", J. Opt. Soc. Amer., Vol. 66, No. 9, September, 1976, pp. 882-92.

5. Rashleigh, S. C., Planar Metal-Clad Dielectric Optical Waveguides, Ph.D. Thesis, University of Queensland, Brisbane, Australia, May, 1975, pp. 190-220.

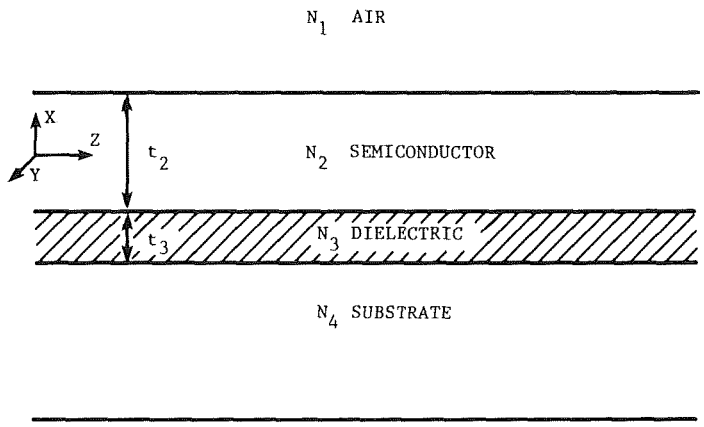

Figure 1.- Four-layer planar waveguide structure.

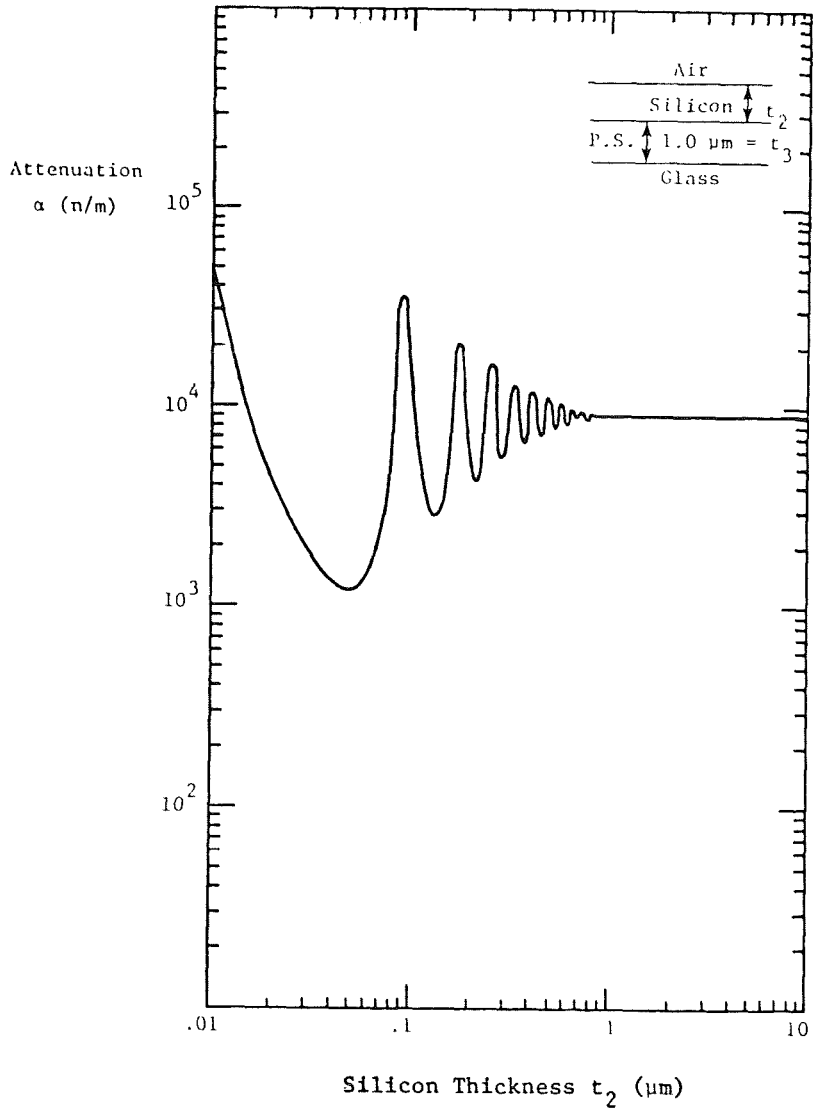

Figure 2.- Attenuation characteristics of silicon-clad waveguide (TE_0 mode, normal conductivity).

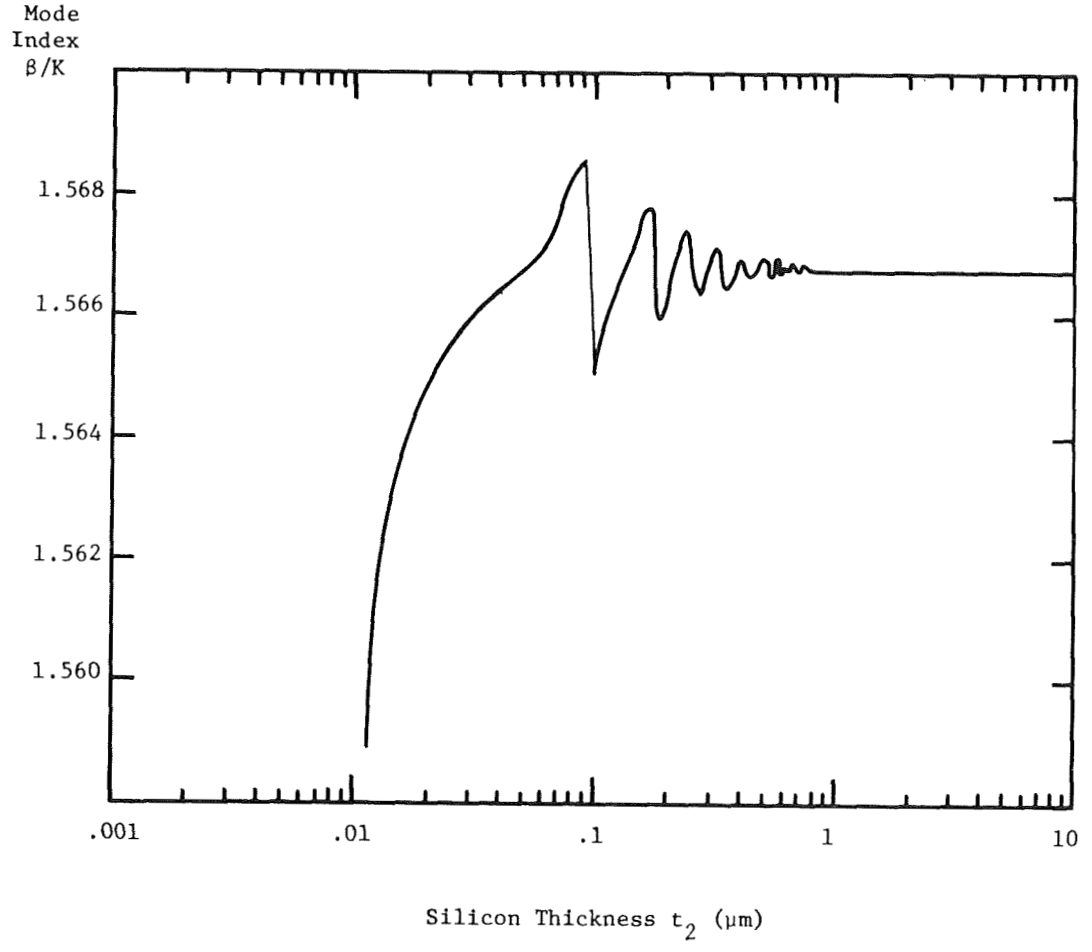

Figure 3.- Mode index characteristics of silicon-clad waveguide (TE_0 mode, normal conductivity).

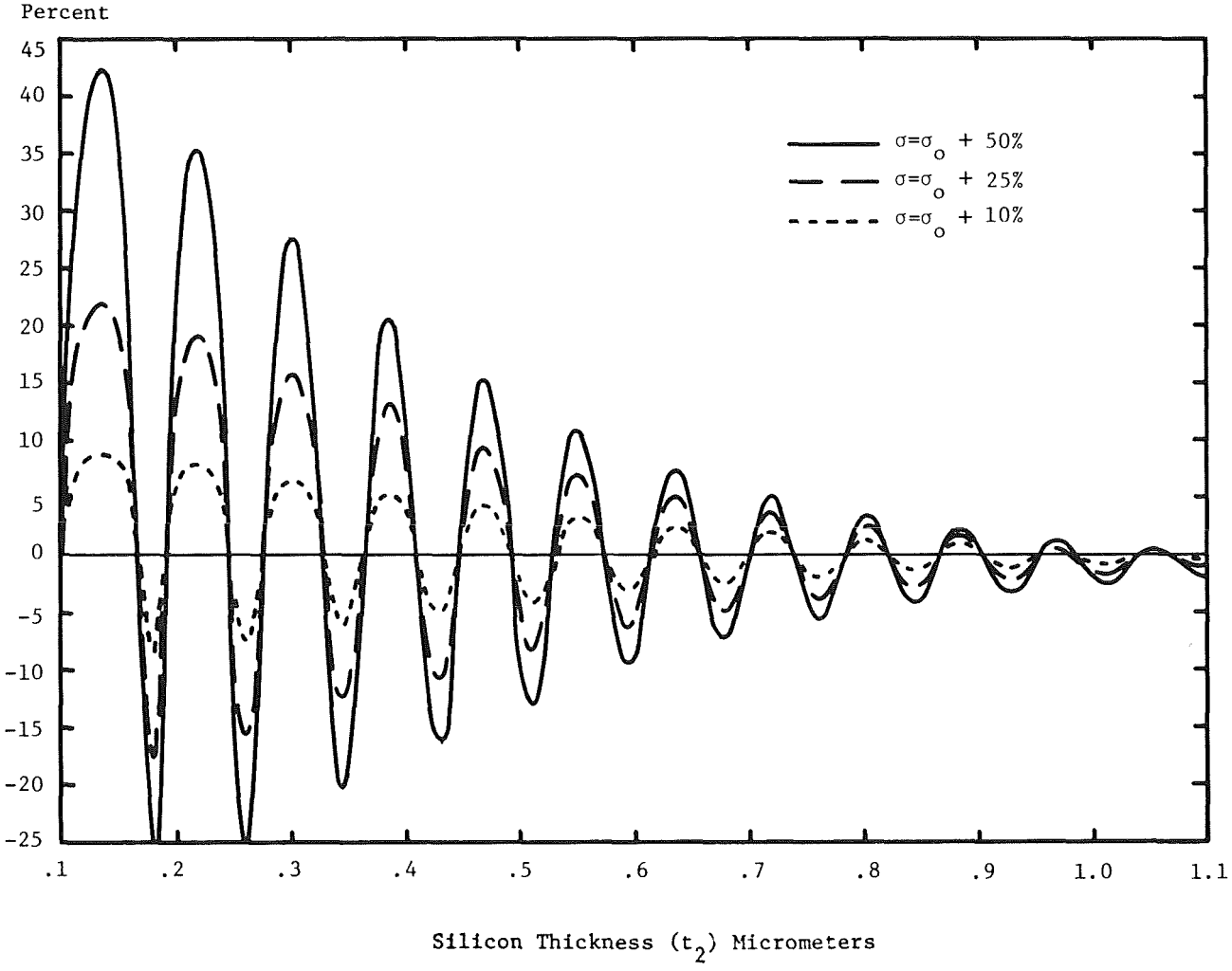

Figure 4.- Change in attenuation with relative change in conductivity (σ_o).

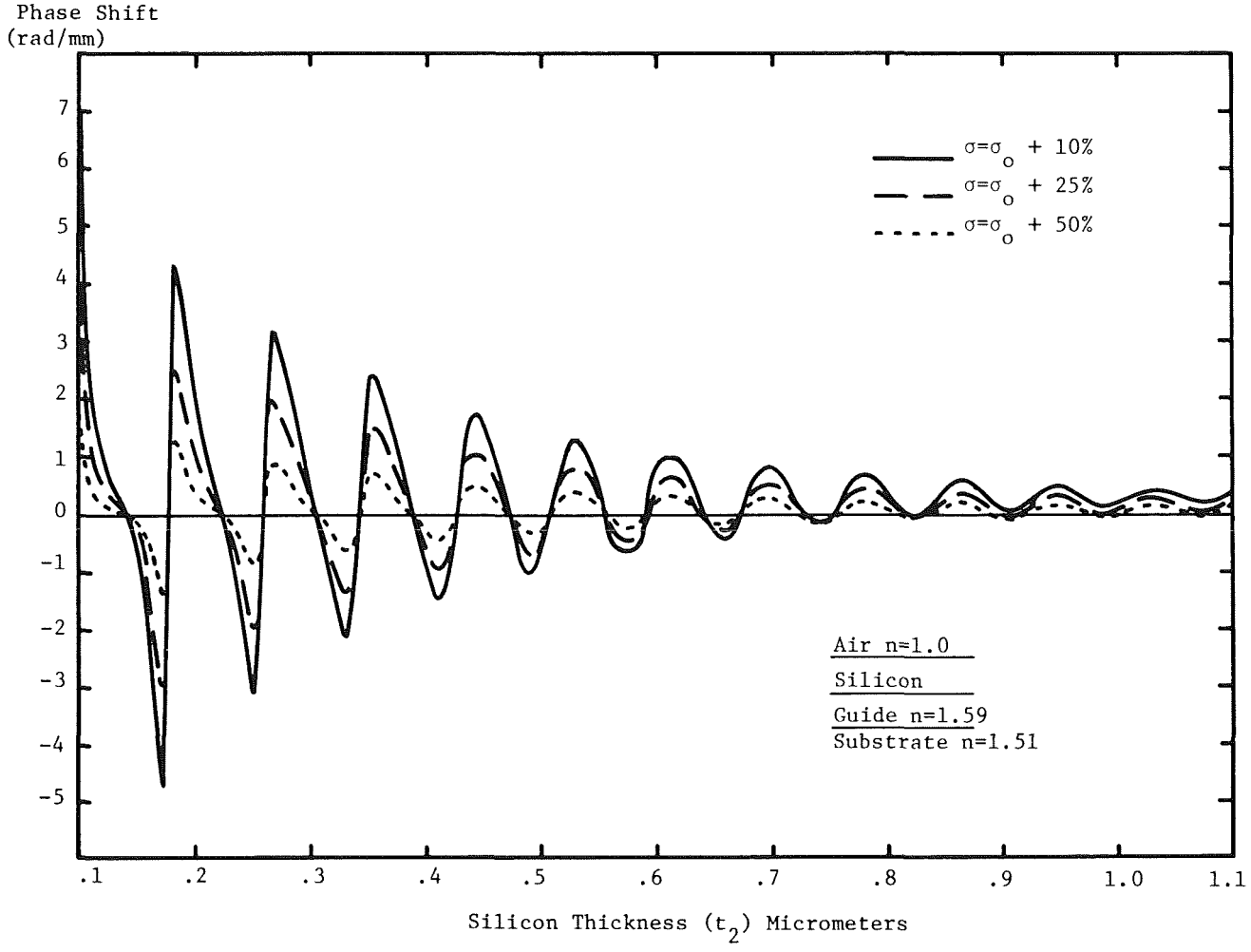

Figure 5.- Change in mode index with relative change in conductivity (σ_o).

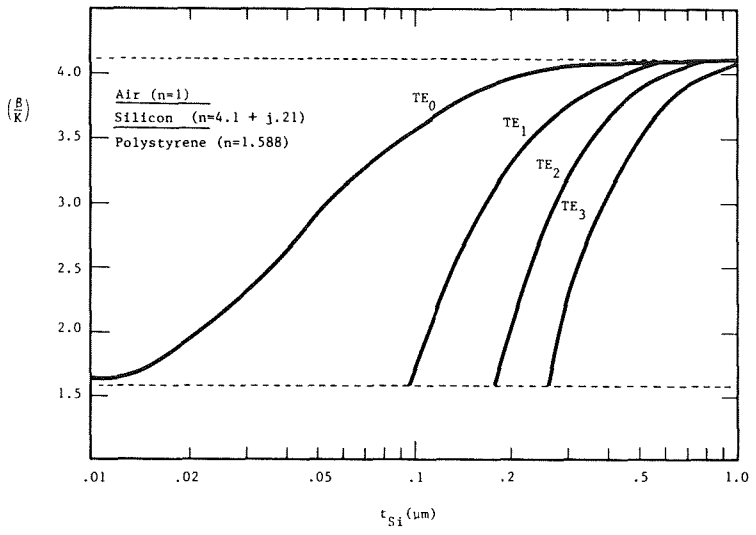

Figure 6.- Attenuation characteristics of silicon waveguide.

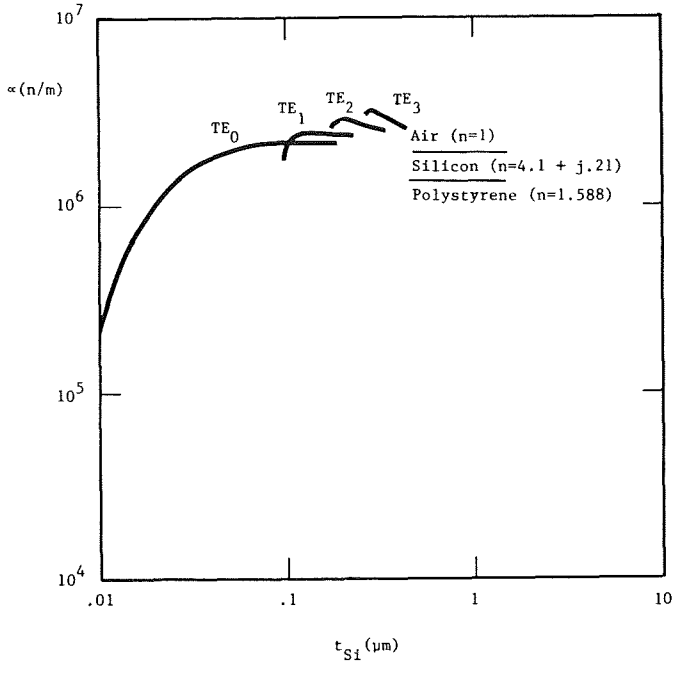

Figure 7.- Mode index characteristics of silicon waveguide.

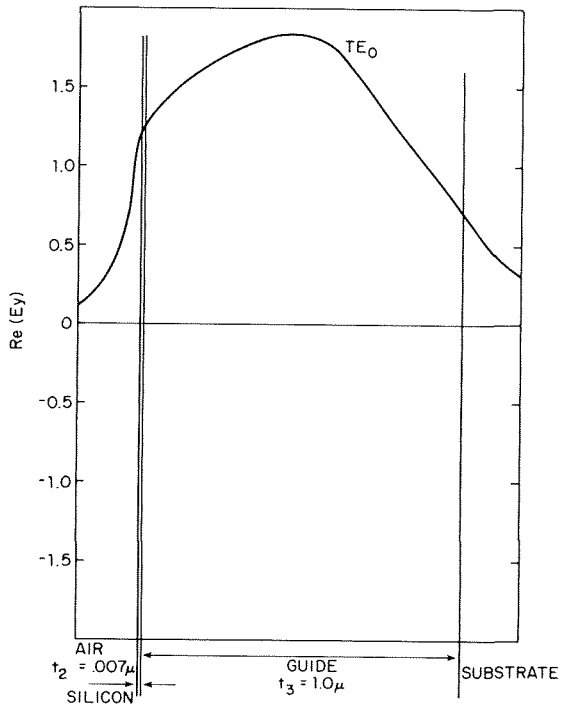

(a) t_{Si} = 0.007μm (below cutoff).

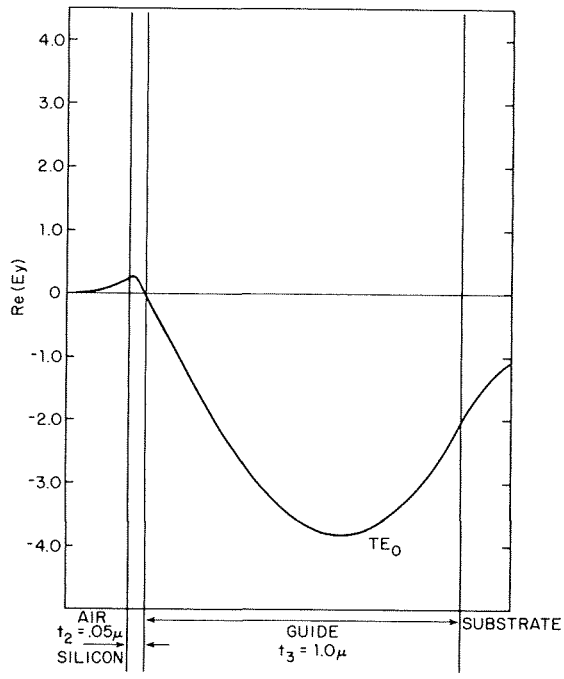

(b) t_{Si} = 0.05μm (local minimum).

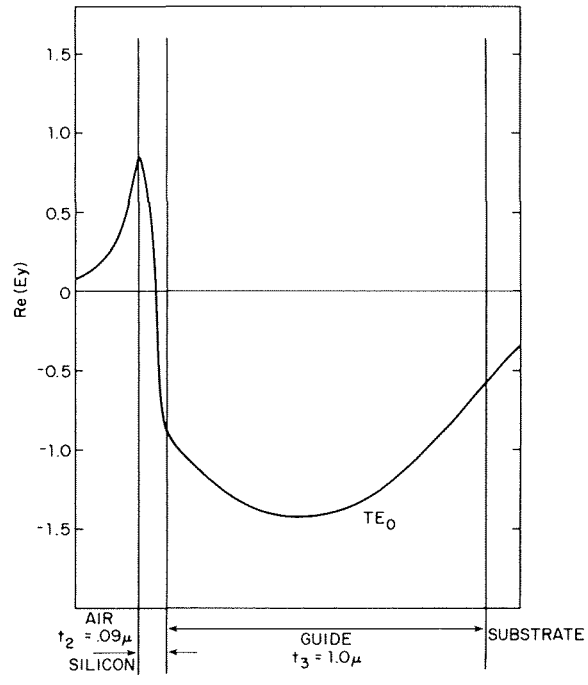

(c) t_{Si} = 0.09μm (local maximum).

Figure 8.- Wave function profile.

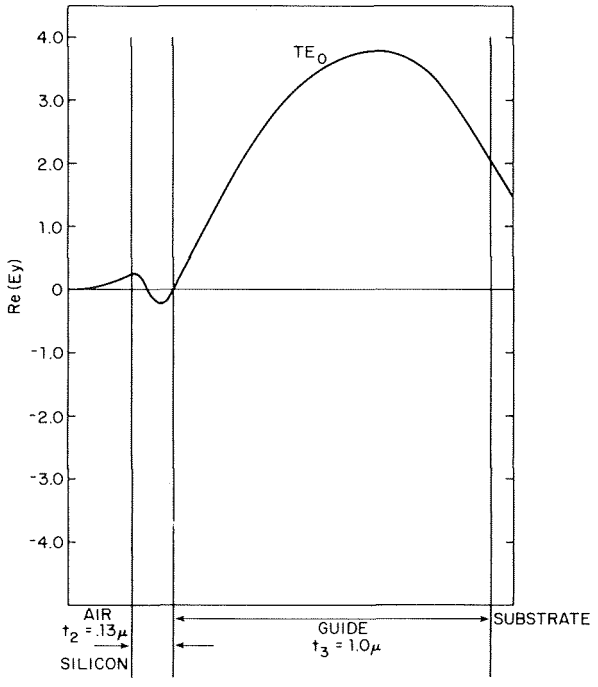

(a) t_{Si} = 0.13μm (local minimum).

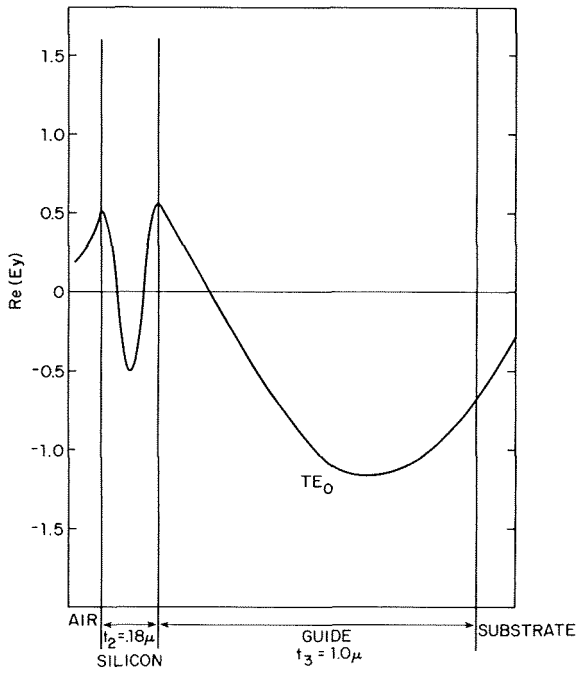

(b) t_{Si} = 0.18μm (local maximum).

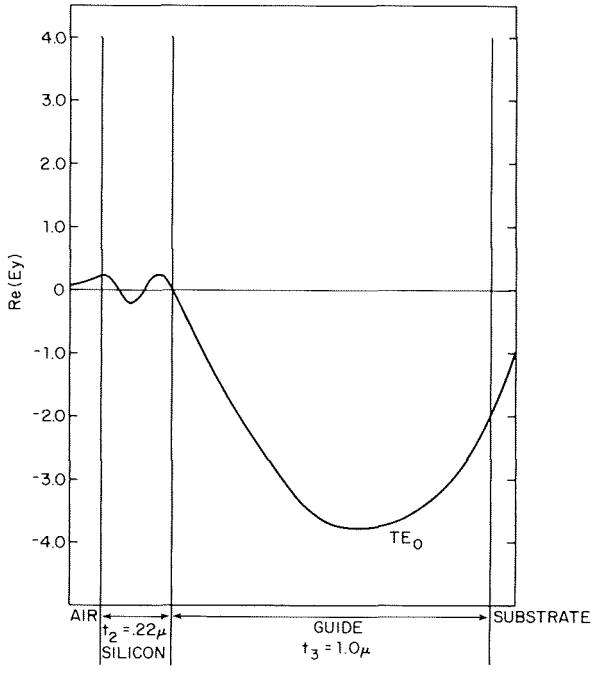

(c) t_{Si} = 0.22μm (local minimum).

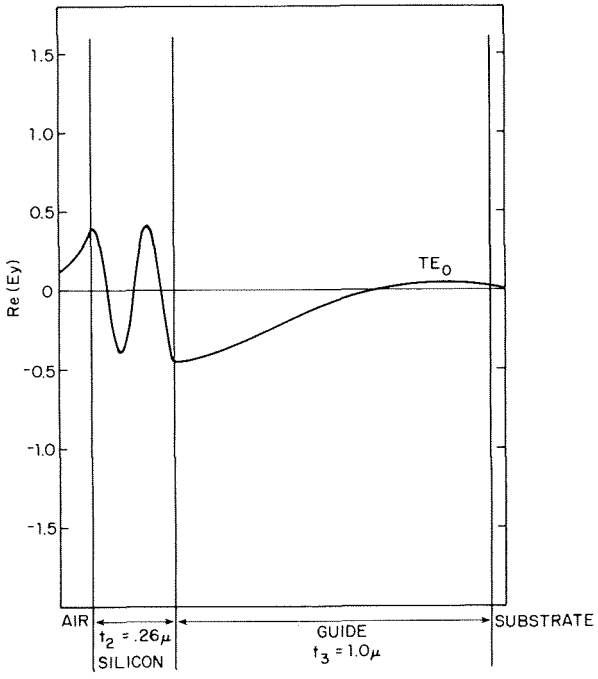

(d) t_{Si} = 0.26μm (local maximum).

Figure 9.- Wave function profile.

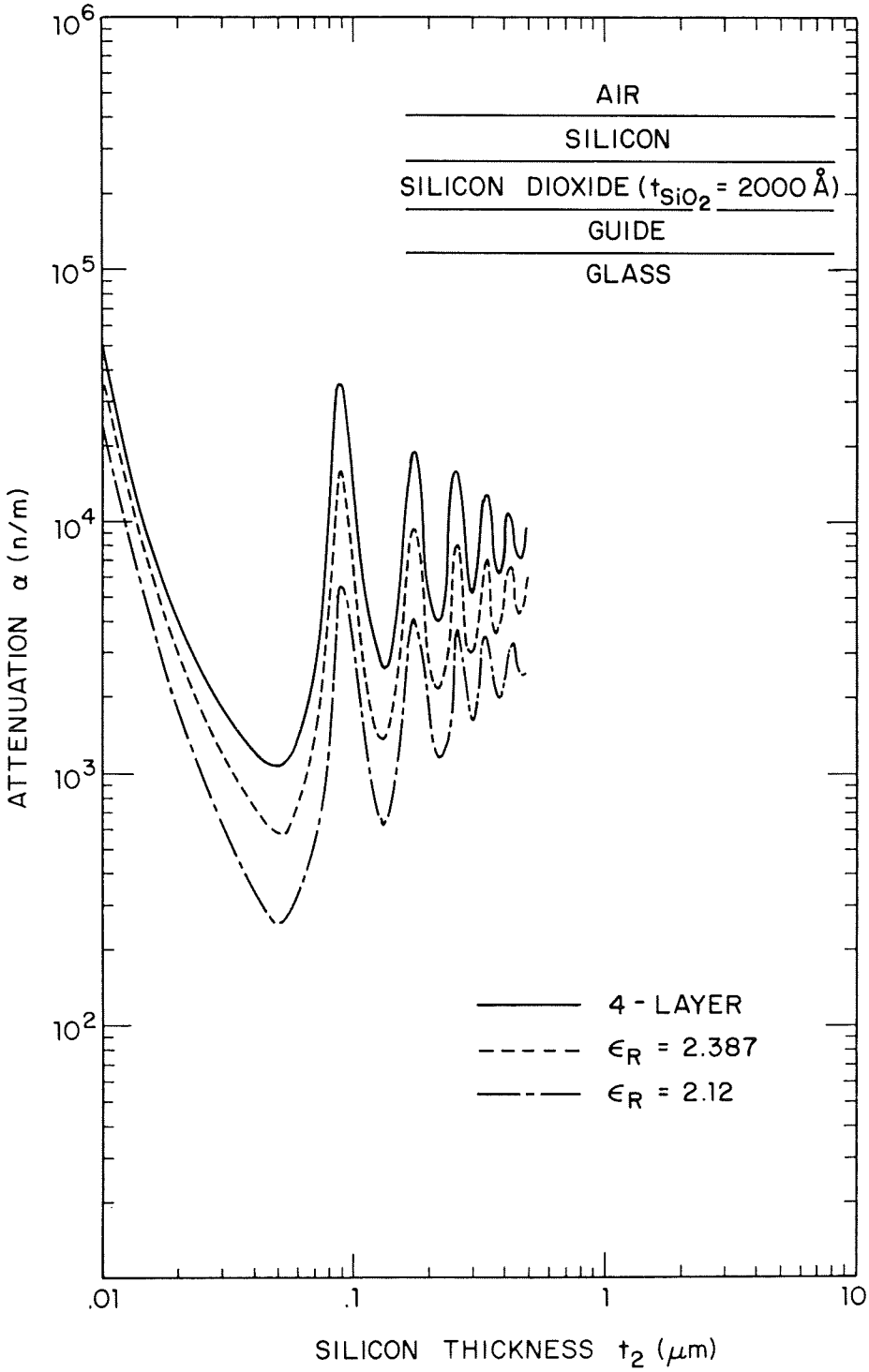

Figure 10.- SiO_2 buffer layer (ε_r = 2.12) of different thicknesses.

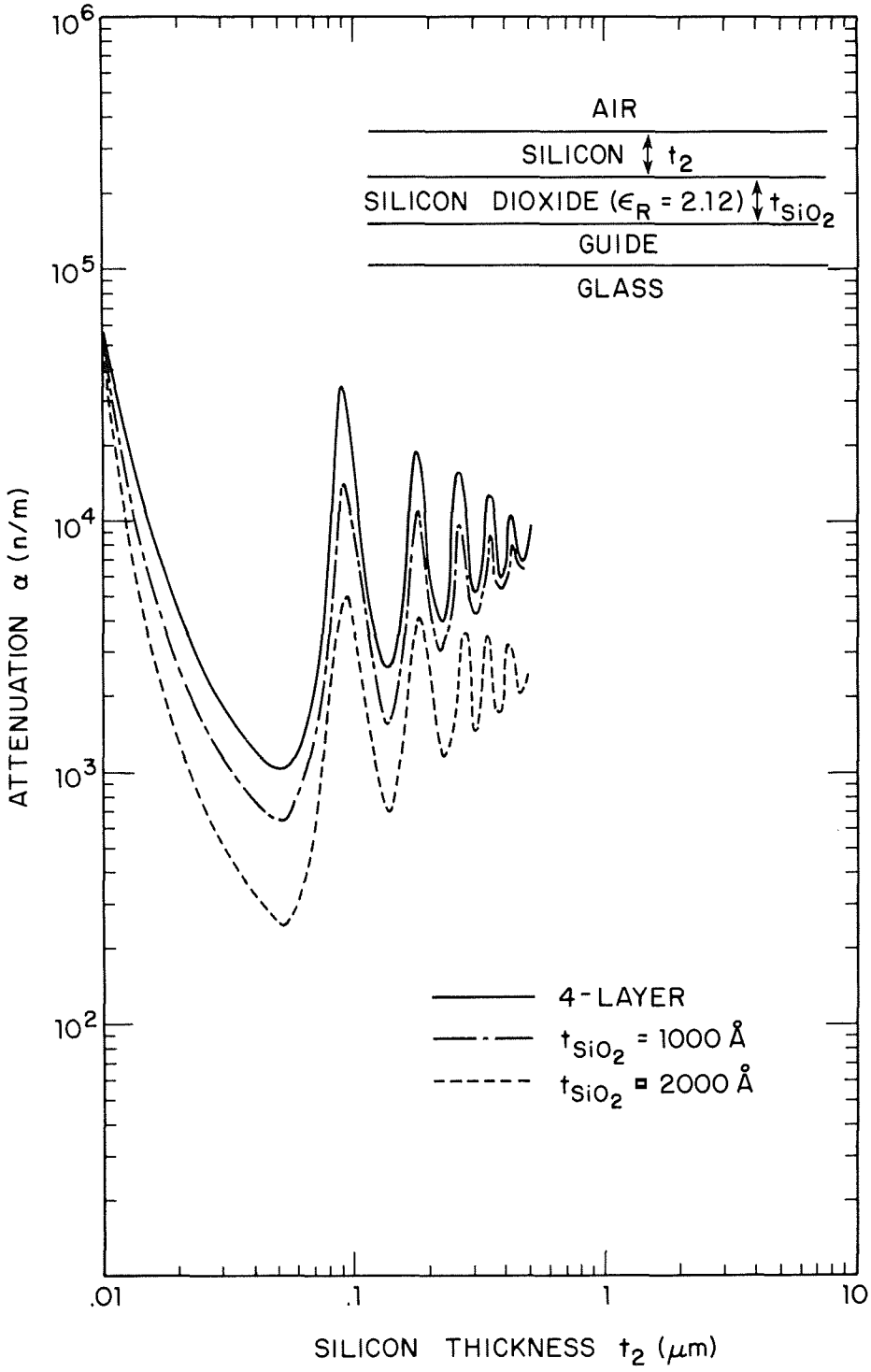

Figure 11.- SiO_2 buffer layer (t_{SiO_2} = 2000Å) of different permittivities.